Enzyme Models

DOI: 10.1002/anie.200604219

Experimental and Theoretical Evidence for Nonheme Iron(III) Alkylperoxo Species as Sluggish Oxidants in Oxygenation Reactions**

Mi Sook Seo, Takashi Kamachi, Tomohisa Kouno, Koji Murata, Mi Joo Park, Kazunari Yoshizawa, and Wonwoo Nam**

The nature of the reactive intermediates in the catalytic oxygenation of hydrocarbons by heme and nonheme iron enzymes has been the subject of intense research in bioinorganic and biological chemistry.[1,2] In cytochrome P450 enzymes (CYP450), high-valent iron(IV) oxo porphyrin π-cation radicals, the so-called Compound I, have been considered as the sole active oxidant that effects oxygenation of hydrocarbons.[1] Similarly, high-valent iron(IV) oxo species have been invoked as reactive intermediates in nonheme iron enzymes.[2] In biomimetic studies, synthetic iron(IV) oxo complexes of heme and nonheme ligands have shown reactivity in a variety of oxygenation reactions.[3,4] Thus, there is no doubt that high-valent iron(IV) oxo species are involved in oxygenation by heme and nonheme iron monooxygenases and their model compounds.

Recent studies from several laboratories, however, have provided indirect evidence that, in addition to high-valent iron oxo intermediates, iron–oxidant adducts **1** also participate in the oxygenation reactions catalyzed by heme and nonheme iron enzymes.[5] A proposed mechanism for the involvement of **1** as a "second electrophilic oxidant" in oxygen-transfer reactions is depicted in Scheme 1; there is competition between oxygen-atom transfer from **1** to organic substrates (pathway A) and conversion of **1** to high-valent iron oxo species **2** through O–X bond cleavage (pathway B). As part of our ongoing efforts to understand the nature of the reactive intermediates involved in oxygenation reactions,[6,7] we investigated the reactivity of mononuclear nonheme iron(III) alkylperoxo species in the oxygenation of organic substrates.

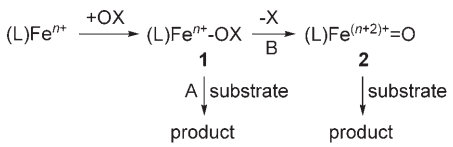

Scheme 1. Plausible intermediates in oxygenation reactions.

The nature of the active oxidant(s) involved in the catalytic oxygenation of organic substrates by nonheme iron complexes and alkyl hydroperoxides has been controversial and remains elusive.[8] In the present study, we prepared nonheme iron(III) alkylperoxo complex [(tpa)Fe^{III}-(OO*t*Bu)]$^{2+}$ (**3**, tpa = tris(2-pyridylmethyl)amine)[9] and studied its reactivity with various organic substrates under stoichiometric conditions by monitoring spectral changes of the intermediate with a UV/Vis spectrophotometer. Complex **3** decayed slowly under the conditions ($k_{obs} = 1.2 \times 10^{-3}$ s^{-1}, Figure S1 of the Supporting Information). Interestingly, the rate of disappearance of **3** was not affected by the presence of substrates such as thioanisole, cyclooctene, cyclooctanol, and triphenylmethane (Table S1 of the Supporting Information), that is, **3** does not react with the substrates. Recently, we similarly reported that nonheme iron(III) hydroperoxo complexes do not react with sulfides and olefins.[7]

Since it was shown recently that addition of an exogenous Lewis base accelerates the conversion of **3** to [(tpa)Fe^{IV}=O]$^{2+}$ (**4**) and enhances the yield of **4**,[9] we added pyridine *N*-oxide to a solution containing **3** and cyclooctene. In this reaction, rapid conversion of **3** to **4** (Figure 1a) was followed by a slow conversion of **4** to the starting [(tpa)Fe^{II}]$^{2+}$ complex (Figure 1b). Furthermore, the conversion of **3** to **4** was not affected by the presence of substrates (data not shown), but the rate of disappearance of **4** was markedly influenced by the presence and nature of substrates (Figure S2 of the Supporting Information). The intermediate **4** was stable for several hours in the absence of substrates, and the rate of reaction of **4** with substrates decreased in the order thioanisole > cyclooctene > cyclooctanol. We have shown previously that **4** reacts with these substrates to give corresponding oxygenated products.[4b–e] In conclusion (Scheme 2), we have provided the first direct spectroscopic evidence that iron(III) alkylperoxo species are not capable of oxygenating organic substrates and that a high-valent iron(IV) oxo complex, generated by O–O bond homolysis of Fe^{III}–OOR,[9] is the active oxidant that oxygenates organic substrates.[8e]

[*] T. Kamachi, T. Kouno, K. Murata, Prof. Dr. K. Yoshizawa
Institute for Materials Chemistry and Engineering
Kyushu University
Fukuoka 812-8581 (Japan)
Fax: (+81) 92-642-2735
E-mail: kazunari@ms.ifoc.kyushu-u.ac.jp
Dr. M. S. Seo, M. J. Park, Prof. Dr. W. Nam
Department of Chemistry
Division of Nano Sciences and Center for Biomimetic Systems
Ewha Womans University
Seoul 120-750 (Korea)
Fax: (+82) 2-3277-4441
E-mail: wwnam@ewha.ac.kr

[**] This research was supported by KOSEF/MOST through Creative Research Initiative Program (W.N.), Grants-in-Aid (No. 18350088, 18GS02070005, and 18066013) for Scientific Research from JSPS (K.Y.), the Nanotechnology Support Project of MEXT (K.Y.), the Joint Project of Chemical Synthesis Core Research Institutions of MEXT (K.Y.), CREST of Japan Science and Technology Cooperation (K.Y.), a Grant-in-Aid (No. 18750048) for Young Scientists from JSPS (T.K.), and the AmorePacific R&D Center (M.J.P.).

Supporting information for this article is available on the WWW under http://www.angewandte.org or from the author.

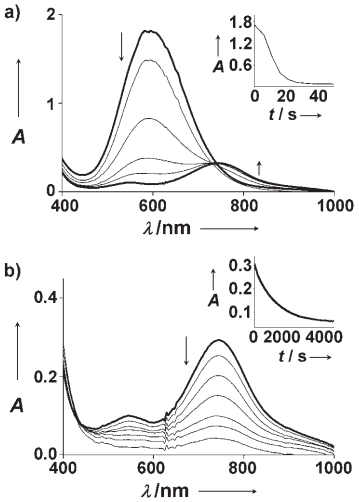

Figure 1. UV/Vis spectral changes for a) the conversion of **3** into **4** on addition of pyridine *N*-oxide and b) the decay of **4** to $[(tpa)Fe^{II}]^{2+}$ in the presence of cyclooctene. Insets show absorbance traces monitored at a) 595 nm for **3** and b) 745 nm for **4**. Reaction conditions: complex **3** was prepared by treating $[(tpa)Fe](ClO_4)_2$ (1 mM) with 2 equiv *t*BuOOH in CH_3CN at −40 °C. Then, cyclooctene (100 mM) was added to the solution of **3**, followed by the addition of pyridine *N*-oxide (12 mM) to the resulting solution.

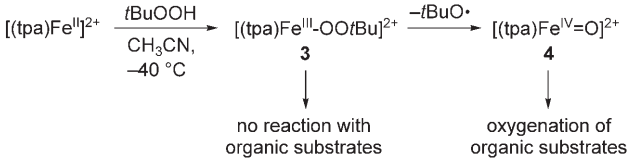

Scheme 2. Iron(III) alkylperoxo and iron(IV) oxo intermediates in oxygenation reactions.

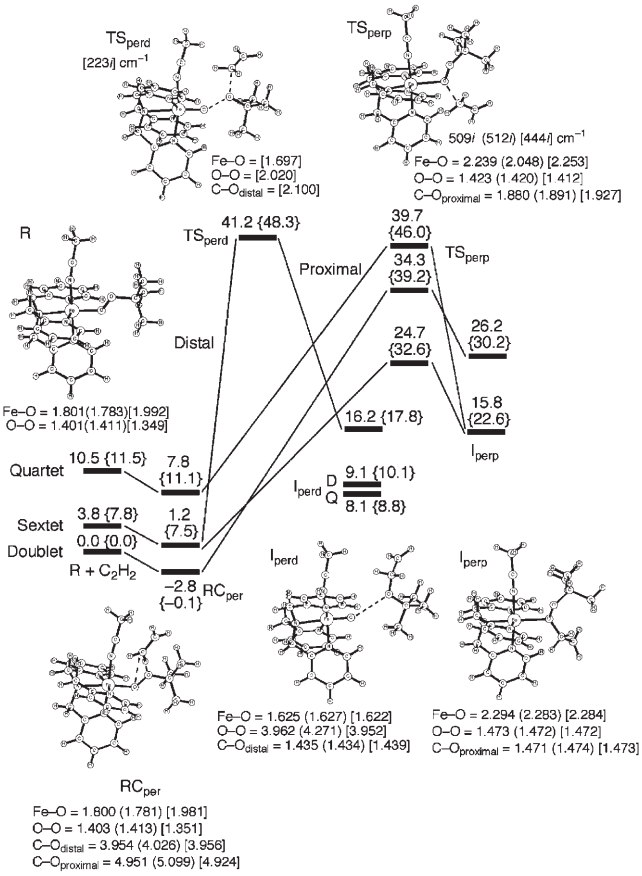

Figure 2. Energy diagrams for ethylene epoxidation by **3**-CH_3CN in the doublet (quartet) [sextet] state. Energies in curly brackets include solvation correction (using a dielectric constant of $\varepsilon = 35.7$ for acetonitrile). Energies in kcal mol^{-1} and bond lengths in Å.

The reactivity of $[(tpa)Fe^{III}(OO\mathit{t}Bu)(CH_3CN)]^{2+}$ (**3**-CH_3CN) in ethylene epoxidation was computed (Figure 2).[10] Detailed data on optimized geometries are collected in the Supporting Information. Iron(III) alkylperoxo species R forms reactant complex RC_{per} with ethylene, and this is followed by a transition state for distal oxygen attack (TS_{perd}) or for proximal oxygen attack (TS_{perp}).[11–13] In TS_{perd}, the O–O bond of the alkylperoxo ligand is cleaved and the distal oxygen atom is transferred to one of the carbon atoms of ethylene. The activation energy for TS_{perd} is 44.0 kcal mol^{-1} in the sextet state when measured from the ground doublet state of RC_{per}; this value is rather high for olefin epoxidation. Such a transition state was not achieved in the doublet and quartet states. The activation energy for proximal oxygen attack in the sextet state is 27.5 kcal mol^{-1} relative to the ground doublet state of RC_{per}; this value is significantly lower than that of TS_{perd}. However, this energy is still higher than that for the O–O bond activation step of **3**-CH_3CN (see below). In conclusion, **3**-CH_3CN does not participate in olefin epoxidation due to the high energy barriers of the pathways for distal and proximal oxygen attack.

We then calculated activation energies for the generation of iron(IV) oxo species $[(tpa)Fe^{IV}(O)(CH_3CN)]^{2+}$ (**4**-CH_3CN) through O–O bond homolysis of **3**-CH_3CN and the ethylene epoxidation by **4**-CH_3CN (Figure 3). Detailed data on the transition-state search for O–O bond homolysis are collected in Tables S2–S4 of the Supporting Information. The energy required for this step was computed to be only 23.5 kcal mol^{-1} on the doublet potential-energy surface, which is in good agreement with the previously reported data of Lehnert et al.[14] The $(CH_3)_3CO^{\bullet}$ moiety of the radical intermediate ($I_{O\text{-}O}$) is then replaced by ethylene in the course of the reaction to form the reactant complex (RC). Formation of a covalent bond between the oxo ligand and a carbon atom of ethylene via $TS1_{C\text{-}O}$ yields $I_{C\text{-}O}$.[15] An activation barrier of 9.9 kcal mol^{-1} is nearly identical to that of ethylene epoxidation by Compound I of CYP450 (9.3 kcal mol^{-1} in the quartet state),[11b] that is, the nonheme iron oxo species has sufficient power to oxidize olefins.[4b] The lifetime of $I_{C\text{-}O}$ is expected to be very short because of the low activation energy for the following ring closure (Table S5 of the Supporting Information), as seen in alkane hydroxylation by nonheme iron(IV) oxo complexes.[16]

We also calculated ethylene epoxidation by $[(tpa)Fe^{III}(OO\mathit{t}Bu)$(pyridine *N*-oxide)$]^{2+}$ (**3**-pyridine *N*-oxide) in the

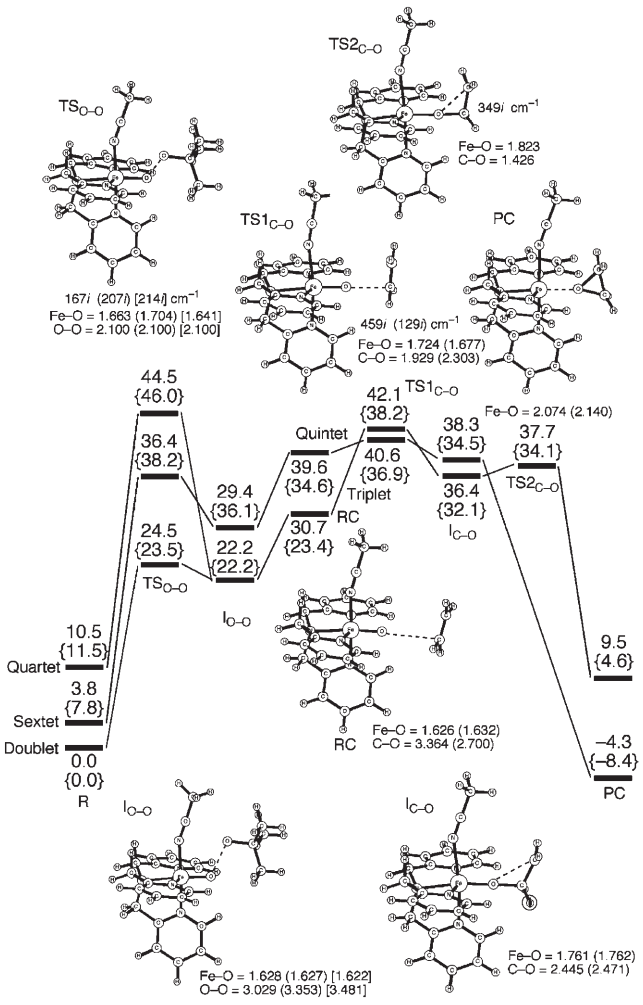

Figure 3. O–O bond activation of **3**-CH_3CN in the doublet (quartet) [sextet] state and ethylene epoxidation by **4**-CH_3CN in the triplet (quintet) state. Energies in curly brackets include solvation correction (using a dielectric constant of $\varepsilon = 35.7$ for acetonitrile). Energies in kcal mol^{-1} and bond lengths in Å.

presence of pyridine *N*-oxide (see above). The energy profile shown in Figure S3 of the Supporting Information is essentially identical to that of ethylene epoxidation by **3**-CH_3CN (Figure 2). Interestingly, the activation energy of the O–O bond homolysis of **3**-pyridine *N*-oxide (21.7 kcal mol^{-1}, Figure S3 of the Supporting Information) is 2.8 kcal mol^{-1} lower than that of **3**-CH_3CN (24.5 kcal mol^{-1}, Figure 3), which is consistent with the experimental result that the addition of pyridine *N*-oxide accelerates the conversion of **3** to **4** (compare Figure 1a for the reaction of **3**-pyridine *N*-oxide with Figure S1 of the Supporting Information for the reaction of **3**-CH_3CN). Furthermore, the calculations indicate that the rate-determining step is the oxidation of ethylene by $[(tpa)Fe^{IV}(O)(CH_3CN)]^{2+}$ (**4**-pyridine *N*-oxide; Figure S3 of the Supporting Information). This prediction matches with the experimental result that conversion of **3** to **4** is much faster than oxidation of cyclooctene by **4** (Figure 1).

In summary, reactivity and spectroscopic studies on a mononuclear nonheme iron(III) alkylperoxo complex revealed that this intermediate is not capable of oxygenating substrates and that a high-valent iron(IV) oxo intermediate, which is generated through O–O bond homolysis of the Fe^{III}–OOR species, is the active oxidant that effects the oxygenation of organic substrates. These experimental results are strongly supported by DFT calculations, in which the energy barrier for O–O bond activation of Fe^{III}–OOR species is lower than that for direct oxygen-atom transfer from the intermediate to organic substrates. Recent DFT calculations on cytochrome P450 reactions revealed that Fe^{III}–OOH is a sluggish oxidant and that the oxidizing power of this species cannot compete with that of a high-valent iron(IV) oxo porphyrin π-cation radical intermediate.[17]

Received: October 16, 2006
Published online: February 16, 2007

Keywords: density functional calculations · enzyme models · iron · oxo ligands · oxygenation

[1] a) P. R. Ortiz de Montellano, *Cytochrome P450: Structure, Mechanism, and Biochemistry*, 3rd ed., Kluwer Academic/Plenum Publishers, New York, **2005**; b) I. G. Denisov, T. M. Makris, S. G. Sligar, I. Schlichting, *Chem. Rev.* **2005**, *105*, 2253; c) B. Meunier, S. P. de Visser, S. Shaik, *Chem. Rev.* **2004**, *104*, 3947.

[2] a) M. L. Neidig, E. I. Solomon, *Chem. Commun.* **2005**, 5843; b) M. M. Abu-Omar, A. Loaiza, N. Hontzeas, *Chem. Rev.* **2005**, *105*, 2227; c) A. Decker, E. I. Solomon, *Curr. Opin. Chem. Biol.* **2005**, *9*, 152; d) S. V. Kryatov, E. V. Rybak-Akimova, S. Schindler, *Chem. Rev.* **2005**, *105*, 2175; e) A. S. Borovik, *Acc. Chem. Res.* **2005**, *38*, 54; f) M. Costas, M. P. Mehn, M. P. Jensen, L. Que, Jr., *Chem. Rev.* **2004**, *104*, 939.

[3] a) J. T. Groves, R. C. Haushalter, M. Nakamura, T. E. Nemo, B. J. Evans, *J. Am. Chem. Soc.* **1981**, *103*, 2884; b) W. Nam, S.-E. Park, I. K. Lim, M. H. Lim, J. Hong, J. Kim, *J. Am. Chem. Soc.* **2003**, *125*, 14674.

[4] a) J.-U. Rohde, J.-H. In, M. H. Lim, W. W. Brennessel, M. R. Bukowski, A. Stubna, E. Münck, W. Nam, L. Que, Jr., *Science* **2003**, *299*, 1037; b) M. H. Lim, J.-U. Rohde, A. Stubna, M. R. Bukowski, M. Costas, R. Y. N. Ho, E. Münck, W. Nam, L. Que, Jr., *Proc. Natl. Acad. Sci. USA* **2003**, *100*, 3665; c) J. Kaizer, E. J. Klinker, N. Y. Oh, J.-U. Rohde, W. J. Song, A. Stubna, J. Kim, E. Münck, W. Nam, L. Que, Jr., *J. Am. Chem. Soc.* **2004**, *126*, 472; d) S. O. Kim, C. V. Sastri, M. S. Seo, J. Kim, W. Nam, *J. Am. Chem. Soc.* **2005**, *127*, 4178; e) N. Y. Oh, Y. Suh, M. J. Park, M. S. Seo, J. Kim, W. Nam, *Angew. Chem.* **2005**, *117*, 4307; *Angew. Chem. Int. Ed.* **2005**, *44*, 4235; f) C. V. Sastri, K. Oh, Y. J. Lee, M. S. Seo, W. Shin, W. Nam, *Angew. Chem.* **2006**, *118*, 4096; *Angew. Chem. Int. Ed.* **2006**, *45*, 3992.

[5] a) W. Nam, Y. O. Ryu, W. J. Song, *J. Biol. Inorg. Chem.* **2004**, *9*, 654; b) L. Que, Jr., *J. Biol. Inorg. Chem.* **2004**, *9*, 684.

[6] W. J. Song, Y. O. Ryu, R. Song, W. Nam, *J. Biol. Inorg. Chem.* **2005**, *10*, 294.

[7] M. J. Park, J. Lee, Y. Suh, J. Kim, W. Nam, *J. Am. Chem. Soc.* **2006**, *128*, 2630.

[8] a) J. Kim, E. Larka, E. C. Wilkinson, L. Que, Jr., *Angew. Chem.* **1995**, *107*, 2191; *Angew. Chem. Int. Ed. Engl.* **1995**, *34*, 2048; b) I. W. C. E. Arends, K. U. Ingold, D. D. M. Wayner, *J. Am. Chem. Soc.* **1995**, *117*, 4710; c) P. A. MacFaul, K. U. Ingold, D. D. M. Wayner, L. Que, Jr., *J. Am. Chem. Soc.* **1997**, *119*, 10594; d) H. Miyake, K. Chen, S. J. Lange, L. Que, Jr., *Inorg. Chem.* **2001**, *40*, 3534.

[9] J. Kaizer, M. Costas, L. Que, Jr., *Angew. Chem.* **2003**, *115*, 3799; *Angew. Chem. Int. Ed.* **2003**, *42*, 3671.

[10] DFT calculations were carried out with the B3LYP hybrid density functional method in combination with the LACVP basis set for the Fe atom and the 6-31G* basis set for the other atoms. See the Supporting Information, Experimental Section for detailed calculation methods.
[11] a) F. Ogliaro, S. P. de Visser, S. Cohen, P. K. Sharma, S. Shaik, *J. Am. Chem. Soc.* **2002**, *124*, 2806; b) T. Kamachi, Y. Shiota, T. Ohta, K. Yoshizawa, *Bull. Chem. Soc. Jpn.* **2003**, *76*, 721.
[12] A. Bassan, M. R. A. Blomberg, P. E. M. Siegbahn, *J. Biol. Inorg. Chem.* **2004**, *9*, 439.
[13] D. Quiñonero, K. Morokuma, D. G. Musaev, R. Mas-Ballesté, L. Que, Jr., *J. Am. Chem. Soc.* **2005**, *127*, 6548.
[14] N. Lehnert, R. Y. N. Ho, L. Que, Jr., E. I. Solomon, *J. Am. Chem. Soc.* **2001**, *123*, 12802.
[15] Although the total barrier starting from R is the same or even larger than that for TS_{perd} and TS_{perp}, O–O bond cleavage and ethylene epoxidation are not directly coupled in energy.
[16] H. Hirao, D. Kumar, L. Que, Jr., S. Shaik, *J. Am. Chem. Soc.* **2006**, *128*, 8590.
[17] E. Derat, D. Kumar, H. Hirao, S. Shaik, *J. Am. Chem. Soc.* **2006**, *128*, 473.

